ENDOR Study of the H Center in LiF†‡

M. L. DAKSS
IBM T. J. Watson Research Center, Yorktown Heights, New York 10598
AND
R. L. MIEHER*
Department of Physics, Purdue University, Lafayette, Indiana 47907
(Received 10 June 1969)

An ENDOR study of the H center in LiF has been performed. Hyperfine constants for 10 sets of nonequivalent neighboring nuclei have been determined by fitting the data with a spin Hamiltonian. The results of this study show that the H center is an F_2^- molecule ion which is oriented along a ⟨110⟩ direction and located on an F^- lattice site, and which is associated with a Na^+ impurity.

I. INTRODUCTION

IT is known that interstitials play a prominent role in the radiation damage of alkali halides, but the structure of these interstitials and their role in the radiation damage is not well understood. The first electron-spin resonance (ESR) study of an interstitial color center in alkali halides was that of the H center by Känzig and Woodruff (KW).[1] These authors suggested from their data that the defect giving rise to the ultraviolet H band in x-irradiated KCl and KBr is a diatomic molecule ion X_2^- of the lattice halide atom X; the molecule ion is located on a halide lattice site with its axis along a [110] crystalline direction, and is equivalent to an interstitial halide atom. ESR data taken by KW in LiF suggested to them that a color center with the same structure appears in x-irradiated LiF (no optical-absorption bands from such a center had previously been observed in LiF).

Observations of the proportionality of H-center and F-center production in KCl during x irradiation at liquid-helium temperatures[2] and of the independence of the production rate of F centers in KCl and KBr on crystal purity[3] (implying an "intrinsic" H center) fit well with the KW H-center model. However, the production of H centers in LiF shows a purity dependence[4,5] (see Sec. II). Further, the LiF H center has a thermal bleaching temperature[4] of approximately 100°K while the KCl and KBr H centers have one of about 60°K. Theoretical results of Dienes *et al.*[6] indicate that H centers of the [110] orientation are unstable in KCl and NaCl if only electrostatic and ion-core repulsive-energy terms in the Hamiltonian are considered; the [111] orientation, with lower energy, is favored. Indeed, this holds true at least qualitatively for the LiF H center, as can be seen by viewing electron density contours.[7] A recent ESR study[7] on a defect generated in highly pure LiF by x irradiation at helium temperatures suggests that that defect is an F_2^- molecule ion centered on a fluoride-ion lattice site and with its molecular axis in a [111] orientation. This model has been verified by an electron-nuclear double resonance (ENDOR) study.[8] The defect bleaches out at about 60°K, and is the intrinsic interstitial defect in LiF.

In this article, we shall describe an ENDOR study of the LiF H center. The ENDOR results prove that this H center consists of an F_2^- molecule ion centered on a halide lattice site and with [110] symmetry, as KW suggested, but is associated with a Na^+ impurity in a nearest-neighbor site (Fig. 1). Experimental details are given in Sec. II. Characteristics of the ESR spectrum are briefly given in Sec. III, as are values obtained for the hyperfine constants of the H-center molecular fluorine nuclei and the anisotropic g factor of the unpaired electron; the values were obtained by fitting the ESR data to a spin Hamiltonian in a rigorous diagonalization technique. The ENDOR data and their analysis are then described in Sec. IV. Besides proving the association, the ENDOR analysis included the determination of hyperfine constants for 10 sets of nonequivalent neighboring nuclei (including the Na^+ nucleus); for this determination, a rigorous spin-Hamiltonian diagonalization technique was used. Conclusions are given in Sec. V.

II. EXPERIMENTAL NOTES

A. Samples Used and Their Preparation

The production rate of H centers in LiF is sample-dependent, as was mentioned in Sec. I. V_K centers[9] (self-trapped holes) are produced together with the H centers under typical conditions, and the V_K ESR lines

† Partially based upon a thesis submitted by M. L. Dakss for the Ph.D. degree at Columbia University.

‡ Work supported by the National Science Foundation, under Grant No. NSF-GP-3385 at Columbia University, and Grant No. NSF-GP-4680 at Purdue University.

* Alfred P. Sloan Fellow.

[1] W. Känzig and T. O. Woodruff, J. Phys. Chem. Solids **9**, 70 (1958).

[2] B. J. Faraday and W. D. Compton, Phys. Rev. **138**, A893 (1965).

[3] H. Rabin and C. C. Klick, Phys. Rev. **117**, 1005 (1960).

[4] W. Känzig, J. Phys. Chem. Solids **17**, 88 (1960).

[5] (a) M. L. Dakss, Ph.D. thesis, Columbia University, 1966 (unpublished). (b) M. L. Dakss and R. L. Mieher, Phys. Rev. Letters **18**, 1056 (1967).

[6] G. J. Dienes, R. D. Hatcher, and R. Smoluchowski, Phys. Rev. **157**, 692 (1967).

[7] Y. Hou Chu and R. L. Mieher, Phys. Rev. Letters **20**, 1289 (1968).

[8] Y. Hou Chu and R. L. Mieher, Phys. Rev. (to be published).

[9] R. Gazzinelli and R. L. Mieher, Phys. Rev. Letters **12**, 644 (1964); Phys. Rev. **175**, 395 (1968).

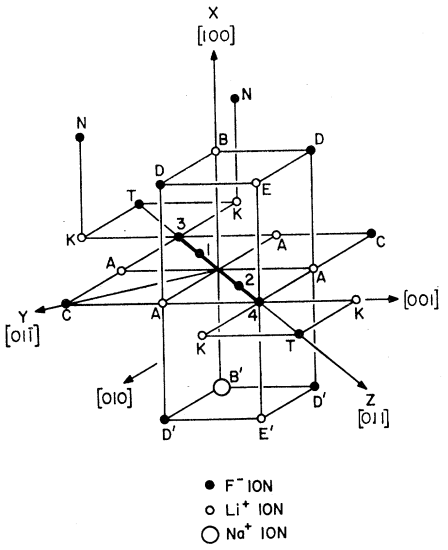

FIG. 1. Lattice model for the H center in LiF.

are much larger in intensity than those of the H center. Since there is overlap between the H- and V_K-center ESR spectra, interpretation of the H-center spectra is hampered. The V_K-center production rate is also sample-dependent, because an impurity is needed to trap the electron freed to make the V_K center. To achieve the maximum H-center production rate while minimizing the corresponding V_K-center production rate, several LiF sample materials were considered. These included Harshaw material of the highest purity available in 1964, and reagent-grade LiF that was in one case undoped and in others doped with Ca, Fe, Na, Mn, Pb, or Tl; the reagent-grade crystals were grown by the Bridgman technique and our examination of them was based on ESR data taken by Bass.[10,11] The material found to give best results was undoped reagent-grade LiF. The high-purity material was irradiated with x rays from a 75-kV and 30-mA machine[9] for 100 h, and on the basis of the lack of any ESR signal above the noise, we concluded that the production rate of H centers in this material was less than a tenth of that in the undoped reagent-grade material.

The samples used for the measurements to be described in this article were in the shape of rectangular parallelpipeds of approximate size 0.20×0.20×0.45 in.; their rotation axis for the angular dependences was along the 0.45-in. dimension. The sample to be used for the rotation in which the dc magnetic field remains in a (100) plane had all surfaces cleaved in (100) planes. The sample used for other rotations had its long dimension in a [110] direction and its long faces in (110) and (100) planes; all faces on this crystal were ground and polished.

[10] I. L. Bass and R. L. Mieher, Phys. Rev. Letters **15**, 25 (1965).
[11] I. L. Bass and R. L. Mieher, Phys. Rev. **175**, 421 (1968).

B. Mounting, Cooling, and Irradiating the Sample; Spectrometer

The Dewar used to keep the sample at a low temperature is a double Dewar very similar to the one described by Gazzinelli and Mieher.[9] Most of the x irradiation[9] was done with liquid nitrogen in the inner Dewar, while ESR and ENDOR data were taken with liquid hydrogen in this Dewar. Since the sample was exposed to room-temperature radiation, the corresponding sample temperatures were approximately 90 and 40°K, respectively. In order to obtain a usable ENDOR signal-to-noise ratio, about 250 h of 75-kV x irradiation were needed. Most ENDOR data were taken with liquid hydrogen in the Dewar, since this gave a nearly optimum signal-to-noise ratio. The ESR and ("stationary") ENDOR measurements were made on an X-band superheterodyne spectrometer operated at 9.430 Gc/sec. The spectrometer and the experimental techniques involved in making measurements have been described previously by Gazzinelli and Mieher.[9]

III. ESR STUDY

A. ESR Spectrum

The ESR spectrum of the H center in LiF has been described by KW. It is characterized by a large anisotropic hyperfine interaction between the unpaired electron and the molecular fluorine nuclei (i.e., the nuclei 1 and 2 in Fig. 1). Because the wave function of the unpaired electron does not spread out very far into the lattice, axial symmetry of the electron wave function is a very good approximation and it is therefore possible to characterize the ESR spectrum by a single angle θ, which $\mathbf{H}_0$ makes with the molecular axis. The hyperfine interaction with the nuclei 1 and 2 produces a "primary splitting" of the ESR spectrum into four lines. The central two lines overlap and do not split resolvably for $\theta \lesssim 75°$; these correspond to the magnetic sublevel $m_{12}=m_1+m_2=0$ of the two nuclei to a good approximation for $\theta \lesssim 75°$ (Sec. III B). The outermost two lines (corresponding to $m_{12}=+1$ and $m_{12}=-1$) are separated by about 1900 G at $\theta=0°$ and move rapidly towards the central lines as θ increases. Because of the hyperfine splitting with the nuclei 3 and 4, each of the lines undergoes a further "secondary splitting" into a four-line spectrum which is a miniature version of the spectrum just described (the separation of outermost lines is here 180 G) and which has a similar angular dependence. We note that KW estimated from the relative hyperfine splittings that the unpaired electron spends about 4 to 10% of its time on the ions 3 and 4.

B. ESR Study

Most of the ENDOR spectra taken in this experiment were taken on an $m_{12}=-1$ ESR line and were influenced significantly by the effect of the hyperfine

interaction between the unpaired electron and the H-center fluorine nuclei 1 and 2 on the electron wave function. Values for the hyperfine constants for these interactions were determined by KW for a sample temperature of 78°K, by fitting their ESR data to a perturbation-theory expression. We have determined these constants using a more rigorous spin-Hamiltonian diagonalization technique and using data taken at the ENDOR sample temperature $T\approx 40$°K. The method used is the same as that used in the ESR study[11] of the V_{KA} center (the V_K center associated with a Li^+ impurity) in NaF. In this technique, the matrix of the spin Hamiltonian is written in a convenient representation. Values for the hyperfine constants and for the anisotropic g factor are assumed. For a series of $\mathbf{H}_0$ orientations, with an assumed trial value of H_0, the matrix elements are evaluated, the matrix diagonalized numerically, and the ESR transition frequency ω_1 calculated from the eigenvalues. For each $\mathbf{H}_0$ orientation, the value of H_0 is corrected until ω_1 agrees with the actual value. The g factor and hyperfine constant components are then varied until, over the angular dependence, the calculated values of H_0 agree with the data within experimental uncertainties. This is an extremely accurate fitting technique.

Since only the hyperfine interaction with the nuclei 1 and 2 was of interest, angular-dependence data were taken only for the ESR lines $m_{12}=1, m_{34}=0$ and $m_{12}=-1, m_{34}=0$, each of which is doubly degenerate. These could be followed only for $0°\leq\theta\lesssim 70°$; outside of this range, these lines are submerged under V_K-center lines and other lines.

The data was fit to the ESR Hamiltonian

$$\mathcal{H}_{\mathrm{ESR}}=\beta_0\mathbf{S}\cdot\mathbf{g}\cdot\mathbf{H}_0+g_0\beta_0\mathbf{S}\cdot\mathbf{T}^{(12)}\cdot\mathbf{I}^{(12)}-\gamma_F\mathbf{H}_0\cdot\mathbf{I}^{(12)}, \quad (1)$$

where $\mathbf{S}$ is the electron spin, $\mathbf{I}^{(12)}=\mathbf{I}^{(1)}+\mathbf{I}^{(2)}$ is the combined spin of the fluorine nuclei 1 and 2, $\mathbf{T}^{(12)}\equiv\mathbf{T}^{(1)}=\mathbf{T}^{(2)}$ is the hyperfine interaction tensor for these nuclei (in gauss) and γ_F (in Mc/sec G) is the fluorine gyromagnetic ratio. The principal-axis system for $\mathbf{T}^{(12)}$ and $\mathbf{g}$ is the XYZ system of Fig. 1. No terms are included in (1) for the nuclei 3 and 4, which have negligible effects in the range $0°\leq\theta\lesssim 70°$. Also, based on results of the V_{KA}-center ESR study,[10,11] in which the positions of the $m_{12}=\pm 1$ lines were found to have a negligible sensitivity in the angular range of interest here to the bent molecular bond caused by the association, it can be shown that bent-bond effects are negligible here too; thus, Eq. (1) does not take them into account.

As in the V_{KA}-center work,[11] the eight-dimensional set of base states are chosen to be of the form

$$|m_S,I^{(12)},m_{12}\rangle=|m_S\rangle|I^{(12)},m_{12}\rangle, \quad (2)$$

where the $|I^{(12)},m_{12}\rangle$ are singlet and triplet states formed from the spins of the nuclei 1 and 2 and where the state $|I^{(34)},m_{34}\rangle=|0,0\rangle$ is assumed. Here $\mathbf{S}$ is quantized along $\mathbf{H}_0$ and $\mathbf{I}^{(12)}$ along the Z axis. As is the case for other F_2^--type centers,[7–12] the analysis shows that the ESR lines of the H center can be well described by the following states $|I^{(12)},m_{12}\rangle$ for $\theta\lesssim 70°$: $|1,1\rangle$ for the low-field line, the combination of $|0,0\rangle$ and $|1,0\rangle$ for the central line, and $|1,-1\rangle$ for the high-field line, which gives meaning to our previous use of m_{12} to describe the lines. Table II of Ref. 11 (with the bond angle set equal to zero) gives the spin-Hamiltonian matrix for the case of $\mathbf{H}_0$ rotated in the YZ plane. The results of the ESR analysis[5a] were (for $T\approx 40$°K): $g_X=2.0115\pm 0.0015$, $g_Y\approx g_X$, $g_Z=2.0013\pm 0.0005$, $|T_X^{(12)}|=75\pm 25$ G, $|T_Y^{(12)}|\approx|T_X^{(12)}|$, $|T_Z^{(12)}|=961.0\pm 0.6$ G.

The sensitivity of the ESR lines to the signs of $T_X^{(12)}$, $T_Y^{(12)}$, and $T_Z^{(12)}$ is less than the experimental uncertainties, so that these signs could not be determined. However, the sensitivity of the ENDOR angular dependences to these signs is also less than experimental uncertainties, making a determination of the signs unnecessary for this analysis. We can note, however, that $T_Z^{(12)}$ is expected to have the same (positive[13]) sign as that for the V_K center in LiF. Bailey[14] has given two separate arguments for a positive sign for $T_X^{(12)}$ and $T_Y^{(12)}$ for the V_K center. One of his arguments made use of the results of theoretical calculations by Das *et al.*[15] of the quantities $T_X^{(12)}$, $T_Y^{(12)}$, and $T_Z^{(12)}$ for the V_K center; these authors (and later Jette[16]) found $T_X^{(12)}$ and $T_Y^{(12)}$ to increase strongly in a positive direction with the amount of overlap of the ions 1 and 2. KW have reported evidence for a larger overlap in the H center in LiF than in the V_K center in LiF; our results (Sec. IV D *2*) are in agreement with this. Thus, the above dependence on overlap would indicate that $T_X^{(12)}$ and $T_Y^{(12)}$ for the H center are greater in a positive direction than those for the V_K center. If we accept Bailey's conclusions on a positive sign for the V_K-center quantities, the H-center quantities would then be positive. The larger absolute magnitudes for the H-center quantities determined in this experiment than for the V_K-center quantities[13] ($|T_X^{(12)}|=|T_Y^{(12)}|=59$ G) support this result.

IV. ENDOR STUDY

A. ENDOR Data

The resolution of ESR in the limited angular range in which data could be taken was not fine enough to show the presence of the impurity association in the H center in LiF (although the V_{KA}-center association could be detected in ESR because of much higher signal-to-noise ratio). The association, however, clearly shows up in ENDOR, both in the appearance of sodium ENDOR

[12] D. F. Daly and R. L. Mieher, Phys. Rev. **175**, 412 (1968).
[13] T. Castner and W. Känzig, J. Phys. Chem. Solids **3**, 178 (1957).
[14] C. E. Bailey, Phys. Rev. **136**, A1311 (1964).
[15] T. P. Das, A. N. Jette, and R. S. Knox, Phys. Rev. **134**, A1079 (1964).
[16] A. N. Jette, Ph.D. thesis, University of California at Riverside, 1964 (unpublished).

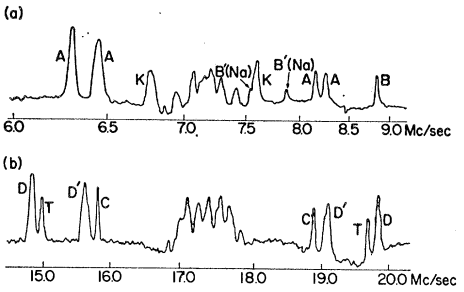

FIG. 2. ENDOR spectrum of the H center in LiF. (a) Lithium and sodium lines; $\mathbf{H}_0$ is approximately along the molecular axis; $T\approx 40°$K; $\gamma_{Li}H_0=7.16$ Mc/sec. The low-frequency lithium B line is not shown. (b) Fluorine lines. Conditions are the same as in (a); $\gamma_F H_0=17.34$ Mc/sec.

lines and in the splitting in other ENDOR lines due to the lower symmetry.

Almost all H-center ENDOR data were taken in the present experiment with H_0 set on the $m_{12}=-1$, $m_{34}=0$ ESR line because it afforded the maximum ENDOR signal-to-noise ratio and because of the simplicity in data interpretation for this line. The simplicity occurs because hyperfine interactions between the unpaired electron and the fluorine nuclei 3 and 4 have a negligible effect on ENDOR data taken for H_0 on this line. No splitting of the ENDOR spectra attributable to the double degeneracy of this ESR line was observed, as was expected based on studies of the V_K-center $m_{12}=0$ lines.[9,11]

ENDOR angular dependences were taken for the following crystal rotations: One in which $\mathbf{H}_0$ moved in the XZ plane of Fig. 1, one in which it moved in the YZ plane, and one in which it moved in a lattice (110) plane with normal making an angle of 60° with the H-center molecular axis. The first two rotations were chosen to provide identification of ENDOR nuclei and to provide data for determination of hyperfine constants; the reflection symmetry of the defect and lattice facilitates doing this.[9] The third, "skew," rotation was performed to aid in nuclear identification.

A typical ENDOR spectrum obtained for the H center in LiF is shown in Fig. 2(a) for the lithium and sodium ENDOR lines and in Fig. 2(b) for the fluorine lines. The ENDOR angular dependences are shown in Figs. 3 and 4. Figure 3 shows the angular dependences for the X-axis rotation [upper panel of Figs. 3(a) and 3(b)] and for the Y-axis rotation (lower panel). The line dividing the two panels in each of Figs. 3(a) and 3(b) corresponds to $\mathbf{H}_0$ along the Z axis, the upper boundary of the upper panel to $\mathbf{H}_0$ along the Y axis, and the lower boundary of the lower panel to $\mathbf{H}_0$ along the X axis. As in previous F_2^- color-center ENDOR studies,[7–12] ξ_X and ξ_Y are used to denote the angles of rotation in the upper and lower panels, respectively. The angle ξ_X is the complement of the more general angle θ defined earlier, while ξ_Y is consistent with θ. Figure 4 shows the experimental ENDOR angular dependences for the skew rotation. The plotted angle θ' of rotation is defined in Fig. 5, in which the H center of interest is along the Z axis while $\mathbf{H}_0$ is rotated in the (110) plane $ABCD$. We note that, when $\theta'=90°$, $\mathbf{H}_0$ is parallel to the YZ plane and makes an angle $\xi_X=45°$ with the defect. Also, when $\theta'=35.2°$, $\mathbf{H}_0$ is parallel to the XZ plane and $\xi_Y=\theta'$. Correlation of the spectra in Fig. 3 with that of Fig. 4 at these two orientations permitted identification of the skew-rotation lines. Data was restricted to $17.5°\leq\theta'\leq 87°$.

We note that for all of the observable ENDOR lines, the contribution of the hyperfine interaction of the nucleus undergoing the transition (the "ENDOR nucleus") to the transition energy is smaller than that of its Zeeman interaction. It then follows[17] that the ENDOR lines always occur in pairs (the members corresponding to the unpaired-electron quantum numbers $m_S=\pm\frac{1}{2}$); the pairs are centered in first order about the frequency $\gamma_n H_0$, where γ_n is the gyromagnetic ratio of the nucleus undergoing the transition. Thus, in all angular-dependence graphs, we use as abscissa not the ENDOR frequency ν but the quantity $\nu-\gamma_n H_0$, to remove the effect of the dependence of H_0 on the crystal orientation. However, in Fig. 3(a) the sodium ENDOR lines are plotted versus $\nu-\gamma_n H_0$, where γ_n is

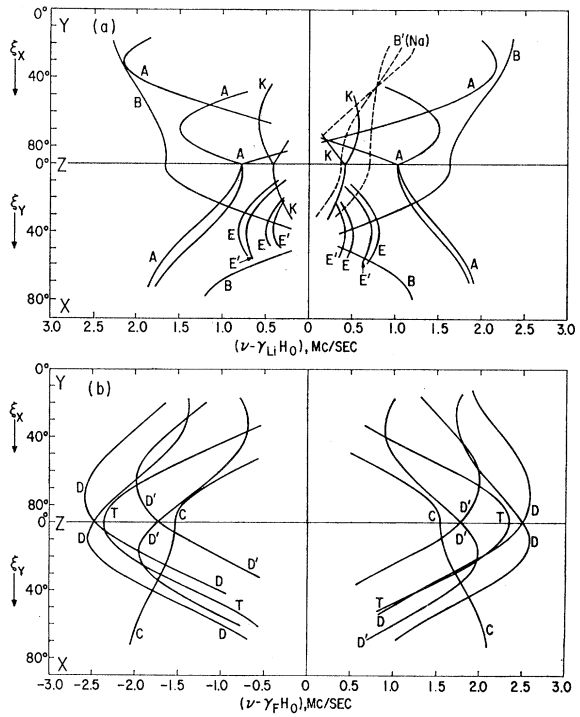

FIG. 3. Experimental ENDOR angular dependence (X- and Y-axis rotations) (a) lithium and sodium lines. Data are plotted as $\nu-\gamma_{Li}H_0$ for both lithium and sodium. (b) Fluorine lines. Data are plotted as $\nu-\gamma_F H_0$.

[17] C. P. Slichter, *Principles of Magnetic Resonance* (Harper and Row, Publishers, Inc., New York, 1963).

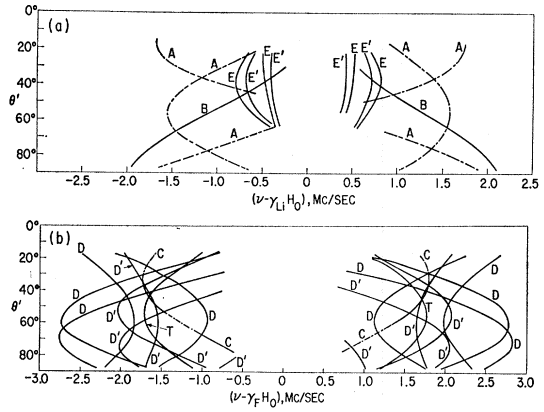

FIG. 4. Experimental ENDOR angular dependences (skew rotation). (a) lithium lines. The angle θ' is defined in Fig. 5, A curve is dashed only when the corresponding ENDOR line exhibits a small splitting (0.1 Mc or less) into two components, and indicates the angular dependence of the center of gravity of the components. (b) fluorine lines. The description is the same as in (a).

that of lithium; this was done so that all lines appeared in their correct relative positions in this plot.

As can be seen in Figs. 2(a) and 2(b), there is a large number of ENDOR lines in the frequency region near the nuclear Zeeman frequencies $\gamma_n H_0$ for lithium and fluorine. These arise from nuclei not in the immediate vicinity of the defect and prevent one from following ENDOR lines from nuclei near the defect when these lines pass through such regions; thus no curves are drawn in these regions in Figs. 3 and 4.

B. Technique for Determination of Hyperfine Constants from Data

The technique used for determining the hyperfine constants of nuclei surrounding the H center from ENDOR data involves the fitting of data to a rigorously diagonalized spin Hamiltonian and is basically the same as that used in the V_{KA}-center ENDOR study[11]; however, modifications were made to treat certain nuclei. We give the Hamiltonian and some definitions here and describe the determination of hyperfine constants in the Appendix. The Hamiltonian used describes the system of the H-center unpaired electron, the fluorine nuclei 1 and 2, and the ENDOR nucleus

$$\mathcal{H}=\mathcal{H}_{\mathrm{ESR}}+\mathcal{H}_{\mathrm{ENDOR}}, \tag{3}$$

where $\mathcal{H}_{\mathrm{ESR}}$ is given in Eq. (1) and where

$$\mathcal{H}_{\mathrm{ENDOR}}=\mathbf{S}\cdot\mathbf{A}\cdot\mathbf{I}-\gamma_n\mathbf{I}\cdot\mathbf{H}_0 \tag{4}$$

includes the hyperfine and Zeeman interactions of the ENDOR nucleus. Effects of the nuclei 3 and 4 and the bent bond can be shown to be negligible and Eq. (3) does not take them into account. All terms in Eqs. (3) and (4) are in units of Mc/sec, as is the hyperfine interaction tensor $\mathbf{A}$. $\mathbf{I}$ is the nuclear spin. No nuclear quadrupole term is included because no significant splitting resulting from quadrupole effects in lithium is observed, and because for sodium we analyze only data taken on the central quadrupole triplet line. Thus, we take $I=\frac{1}{2}$. The hyperfine interaction term of Eq. (4) can be expanded as follows:

$$\mathbf{I}\cdot\mathbf{A}\cdot\mathbf{S}=\mathbf{I}\cdot\mathbf{B}\cdot\mathbf{S}+a\mathbf{I}\cdot\mathbf{S}$$
$$=\sum_{l,m=X,Y,Z}(B_{lm}+a\delta_{lm})I_lS_m, \tag{5}$$

where

$$a\mathbf{I}\cdot\mathbf{S}=(8\pi/3)\gamma_e\gamma_n\hbar^2C_0|\psi(\mathbf{d})|^2\mathbf{I}\cdot\mathbf{S} \tag{6}$$

is the contact (or isotropic) part of the hyperfine interaction, and

$$B_{lm}=\gamma_e\gamma_nC_0\hbar^2\int\left[|\psi(\mathbf{r})|^2\frac{3(r_l-d_l)(r_m-d_m)}{|\mathbf{r}-\mathbf{d}|^5}-\frac{\delta_{lm}}{|\mathbf{r}-\mathbf{d}|^3}\right]d\mathbf{r} \tag{7}$$

are the elements of the dipole-dipole interaction tensor $\mathbf{B}$ in the XYZ system of coordinates. $\mathbf{I}\cdot\mathbf{B}\cdot\mathbf{S}$ is the dipole-dipole or anisotropic part of the hyperfine interaction. $\psi(\mathbf{r})$ is the wave function of the unpaired electron at the position described by the radius vector $\mathbf{r}$ from the origin, and $\mathbf{d}$ is the radius vector drawn from the origin to the nucleus (r and d are in cm units). γ_e and γ_n are the electron and nuclear gyromagnetic ratios, respectively, in units of Mc/sec G; $C_0=10^6/2\pi\hbar$; δ_{lm} is the Kronecker delta. We denote the principal-axis system of A and B as the xyz system and write

$$\mathbf{I}\cdot\mathbf{A}\cdot\mathbf{S}=\sum_{i=x,y,z}A_iI_iS_i=\sum_i(a+B_i)I_iS_i. \tag{8}$$

The quantities A_i and the principal-axis directions comprise the hyperfine constants for the nucleus under consideration.

The technique used to determine hyperfine constants from the ENDOR data is briefly described in the Appendix.

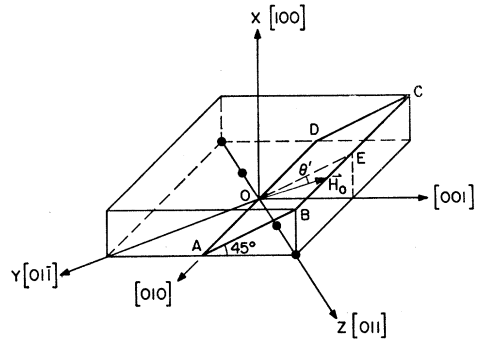

FIG. 5. Explanation of skew rotation. The H center is oriented along the Z axis. $\mathbf{H}_0$ is rotated in the (110) plane $ABCD$. θ' is the angle between $\mathbf{H}_0$ and the [110] direction OE.

C. Techniques for Nuclear Identification

The main technique for identifying ENDOR lines with lattice nuclei involves the use of symmetry considerations.[9] The lattice nuclei surrounding the defect can be divided up into "sets" of nonequivalent nuclei; members of any one set go into one another under the symmetry transformations of the defect and lattice. The principal axes of the hyperfine tensor $\mathbf{A}$ of any two members of a given set are exchanged under the same symmetry transformation that exchanges the positions of the two nuclei, and corresponding principal values are equal. We denote nuclei in the same set by the same label. Nuclei of the same set become "equivalent" if $\mathbf{H}_0$ makes equal angles with corresponding principal axes of these nuclei. ENDOR lines of equivalent nuclei coincide (if interactions between the nuclei are small,[8] as is the case for all nuclei surrounding the H center). The observation of such coincidences permits the correlation of ENDOR lines with nuclei.

The presence of the sodium ion in the H center destroys the inversion symmetry and the reflection symmetry in the YZ plane. This breaks up each set of nonequivalent nuclei not lying in the YZ plane into two smaller sets, lying on either side of this plane. We differentiate between the smaller sets by giving them primed and unprimed labels of the same letter; a primed label corresponds to location on the sodium B' side of the YZ plane. Although ENDOR lines from the two smaller sets have the same equivalence behavior, it is often possible to correlate lines with a particular set by examining the magnitudes of the dipole-dipole hyperfine constants (abbreviated DDHFC's and consisting of the set B_x, B_y, B_z, and principal-axis directions) and the contact interaction hyperfine constants. The experimental hyperfine constants and their contact and DDHFC components are given in Table I (see Sec. IV D *2* for discussion). Since the sodium B' ion is larger in size than a Li^+ ion, it is expected to push the molecule ion towards nuclei on the other side of the YZ plane. This usually leads to larger values for $|a|$, $|B_x|$, $|B_y|$, and $|B_z|$ for these nuclei than for their primed counterparts.

Identification of nuclei was aided in several cases by a comparison of the experimental DDHFC's with those calculated using a computer program developed by Daly and Mieher.[18] This program performs the integration of Eq. (7) numerically, and uses a self-consistent field wave function calculated for the free F_2^- molecule ion by Wahl[19]; details are given in Ref. 18.

Following the technique of Ref. 18, we also make use of the program in an estimate of the displacements Δ of certain neighboring lattice nuclei caused by the presence of the H center and of the spacing R between the molecular fluorine nuclei in the defect. This could be done because wave functions $\psi(\mathbf{r})$ for several values of R were available,[19] so that Δ for a particular nucleus and R could then be varied to obtain the best fit between theoretical and experimental DDHFC's for that nucleus. Displacement estimates are relatively insensitive to the details of the F_2^- wave function,[18] so that lattice effects can be small. The results of such estimates are often useful in nuclear identification; an incorrect nucleus will require an unreasonable displacement. Estimates of R are quite sensitive to wave-function details, but a value of R estimated by fitting the Li B DDHFC's (as calculated from the free molecule-ion wave function) to experiment is fairly accurate because of the insensitivity of the DDHFC's of nodal-plane lithium nuclei to lattice effects.[18] We have made such an estimate with lithium B and obtained $R=3.6$ a.u. (Sec. IV D *2*); we have used this R in calculating DDHFC's of other nuclei for nuclear identification purposes.

D. Results and Discussion

1. Proof of H-Center Model

The ENDOR spectrum of the H center in LiF provided definite proof of the H-center model of Fig. 1. ENDOR lines were identified for the lithium A, B, E, E', and K nuclei, the sodium B' nuclei, and the fluorine C, D, D', and T nuclei in the figure; identification was done primarily by symmetry considerations (Sec. IV C). We describe some of the identifications briefly.

Two lithium E and two lithium E' ENDOR lines on either side of the ENDOR pattern center are expected in the Y-axis rotation and are observed. Throughout the X-axis rotation, the E and E' lines were submerged under other lines in the pattern center and could not be located. Consequently, A_y (where the y axis is along the Y axis) could not be determined from the data, so that a, B_x, B_y, and B_z for these nuclei could not be separated out from the experimental hyperfine constants. To distinguish between the E and E' nuclei, we note that the smaller $|A_x|$ and $|A_y|$ for the lithium E' nuclei probably implies smaller $|B_x|$, $|B_y|$, and $|B_z|$ values and a smaller $|a|$ so that these nuclei are probably on the "primed" side of the YZ plane, as labeled.

The association is expected to cause a splitting of the lithium A lines in the Y axis and skew rotations as well as a splitting of the fluorine C lines in the skew rotation; both splittings are observed in the data. However, splittings of the fluorine T lines would be expected in the Y axis and skew rotations, but none are observed. This lack of a resolvable splitting can be explained by noting that the fluorine F splitting in the NaF V_{KA}-center ENDOR study[11] is quite small (0.1 Mc/sec maximum). The T nuclei of the H center are significantly further from the F_2^- molecule ion than the fluorine nuclei of the V_{KA} center and are expected to show a much smaller splitting.

[18] D. F. Daly and R. L. Mieher, Phys. Rev. Letters **19**, 637 (1967); Phys. Rev. **183**, 368 (1969).

[19] A. C. Wahl (private communication); see also T. L. Gilbert and A. C. Wahl, Bull. Am. Phys. Soc. **10**, 1097 (1965).

TABLE I. Principal-axis (x,y,z) hyperfine constants in Mc/sec, and their contact and dipole-dipole components. The principal-axis orientations α,β,γ are measured with respect to the H-center principal axes X,Y,Z.

Nucleus	A_x	A_y	A_z	α (deg)	β (deg)	γ (deg)	a	B_x	B_y	B_z
A(Li)	−3.93±0.04	−4.34±0.03	−3.00±0.02	∼1	23.5±1.0	23.5±1.0	−0.86	−3.07	5.20	−2.14
B(Li)	2.48±0.04	−4.87±0.04	−3.29±0.02	0	0	0	−1.89	4.37	−2.98	−1.40
B'(Na)	−3.05±0.10	−6.05±0.04	−5.39±0.02	0	0	0	−4.83	1.78	−1.22	−0.56
E(Li)	1.00±0.03	···	−1.62±0.03	46±2	0	46±2	···	···	···	···
E'(Li)	0.83±0.03	···	−1.45±0.03	46±2	0	46±2	···	···	···	···
K(Li)	−0.33±0.12	−0.31±0.12	1.15±0.02	∼0	28±1	28±1	0.17	−0.50	−0.48	0.98
C(F)	−4.33±0.04	1.06±0.11	−3.07±0.02	∼1	∼1	0	−2.11	−2.22	3.17	−0.96
D(F)	−6.81±0.90	2.18±0.60	−5.10±0.10	52±2	53±2	8±2	−3.24	−3.57	5.42	−1.86
D'(F)	−4.67±0.90	2.38±0.60	−3.92±0.10	52±2	54±2	15±2	−2.07	−2.60	4.45	−1.85
T(F)	0.55±0.08	0.54±0.08	4.68±0.02	0	0	∼0	1.92	−1.37	−1.38	2.76

That the ENDOR lines ascribed to the fluorine D and D' nuclei are not actually due to the fluorine D and N nuclei has been shown quite definitely by a DDHFC calculation made by Daly[20] using the technique mentioned in Sec. IV C. He showed that a displacement of a D nucleus by an amount $0.03a_0$ away from the defect (where a_0 is the lattice spacing) yields agreement between the theoretical DDHFC's and those obtained from the ENDOR lines labeled fluorine D in Figs. 3 and 4, while displacement of a D' nucleus by $0.17a_0$ gives agreement with the experimental fluorine D' constants. The unreasonable displacement of about a_0 was found to be required for the fluorine N nucleus to get agreement with the experimental fluorine D' hyperfine constants indicating that these constants could not arise from the fluorine N nuclei.

An important confirmation of an association is the existence of ENDOR lines from the impurity ion. We have observed the sodium B' lines (Fig. 3) on the high-frequency side of $\gamma_{Na}H_0$; the low-frequency lines are submerged in the pattern center. The expected quadrupole splitting[10–12] of these lines is seen; the quadrupole constants were measured from the data to be (in Mc/sec) $Q_{zz}=0.33\pm0.02$, $Q_{yy}=-0.28\pm0.02$, and $Q_{xx}=-(Q_{yy}+Q_{zz})=-0.05\pm0.03$. That these lines come from a sodium nucleus was confirmed by examining the difference between the frequency shift $\Delta\nu_{Na}$ of the sodium lines and that, $\Delta\nu_{Li}$, of nearby lithium lines, going from data taken on the usual $m_{12}=-1$, $m_{34}=0$ ESR line to data taken on the $m_{12}=-1$, $m_{34}=-1$ ESR line, with $\mathbf{H}_0$ parallel to the Z axis. The difference $\Delta\nu_{Na}-\Delta\nu_{Li}$ should be simply $(\gamma_{Na}-\gamma_{Li})(\Delta H_0)$, where $\Delta H_0=89$ G is the change in H_0 going from one ESR line to the other, or $\Delta\nu_{Na}-\Delta\nu_{Li}=0.047$ Mc/sec. The observed value is 0.05 Mc/sec. Another confirmation that the defect is associated with a Na^+ ion, and in fact with one in the B' site, is that the DDHFC's ascribed to sodium B' in Table I are almost identical to those of the sodium A nucleus of the V_{KA} center in NaF and to those of the Na A nucleus of the V_K center in NaF, if the transformations $B_y\rightarrow B_x$ and $B_x\rightarrow B_y$ are made (the sodium A ion in the latter centers are located on the Y, rather than the X axis). The difference $|\Delta B_i|\leq0.01$ in Mc/sec for $i=x$, y, and z occurs in the comparison with the V_{KA} center and the difference $|\Delta B_i|\lesssim0.08$ occurs in the comparison with the V_K center. In fact, it can be shown that an impurity ion located in any position but one on the X axis would lead to a splitting of the lithium A lines in the X-axis rotation into more components than observed; the fluorine C lines would also split in the X- or Y-axis rotations, as is also not observed. Thus, it is quite certain that the impurity is on the X axis. The large separation between the fluorine D and D' ENDOR lines (comparable to the largest ones observed for the closely bound V_{KA} center in NaF[11]) confirms that the Na ion is a nearest neighbor.

We see that all ENDOR angular-dependence behavior predicted by symmetry considerations and DDHFC calculations for an H center with the structure shown in Fig. 1 are observed. It is reasonable to conclude that this structure has been verified.

2. *Hyperfine Constant Determinations and Nuclear Displacement Estimates*

The determination of hyperfine constants by fitting the experimental data to the spin Hamiltonian with the diagonalization techniques of Sec. IV B was relatively straightforward. Generally, available regions of angular dependence most sensitive to a particular hyperfine constant were used in the determination of that constant (e.g., the region near $\theta=0°$ for A_z of fluorine T). The fluorine D and D' hyperfine constants were the only ones requiring the generalized analysis technique of the Appendix. For these nuclei, the treatment was simplified by the assumption that one principal plane of $\mathbf{A}$ was parallel to the Z axis; it is expected[5a] that this plane will be closely parallel to the plane passing through the Z axis and the D nucleus.

The hyperfine constant results for all the nuclei are given in Table I. For all but the fluorine D and D' nuclei, the theoretical angular-dependence curves derived from

[20] D. F. Daly (private communication).

these hyperfine constants agreed with almost all experimental points within experimental uncertainties; these uncertainties usually varied from about ± 0.01 Mc/sec near $\theta=0°$ to about ± 0.03 Mc/sec near $\theta=70°$. For the fluorine D and D' nuclei, discrepancies were often up to two or three times experimental uncertainties, but this could be explained by the assumption made restricting one principal plane to parallelism to the Z axis.

The displacement-internuclear spacing determination technique described in Sec. IV C was applied to the lithium B nucleus. The results were a displacement $\Delta_{\mathrm{Li}}=-0.023a_0$ along the X axis and an internuclear spacing $R=3.6$ a.u. In a study[18] of the V_K center in LiF in which the DDHFC's of a nodal-plane lithium nucleus were similarly fitted to experiment, the value $R=3.8$ a.u. was determined. The smaller R for the H center is consistent with conclusions of KW based on hyperfine splitting, g shift, and optical-absorption data.

Making use of curves obtained in a displacement-internuclear spacing study[18] of the V_{KA} center in NaF, we determine for the LiF H center the values $\Delta_{\mathrm{Na}}=0.16a_0\hat{X}$ for the sodium B' nucleus and $R=4.3$ a.u. The large difference between the results for R in the lithium B and sodium B' calculations is partially due to the distortion of the F_2^- molecule ion caused by the association. Because of such effects as exchange polarization of F_2^- closed-shell molecular orbitals, which are important[18] for the sodium B' nucleus but not for the lithium B nucleus, the value $R=3.6$ a.u. is expected to be the more accurate of the two. The displacements Δ_{Li} and Δ_{Na} are relatively insensitive to the wave-function details and are probably consistent estimates.[18] Note that the displacements are measured relative to the molecule ion's position; thus the negative displacement for the lithium B probably means that both the F_2^- and the lithium B were pushed away from the sodium B' but ended up closer to one another by $0.023a_0$. It is of interest to compare the difference $\Delta_{\mathrm{Na}}-\Delta_{\mathrm{Li}}=0.18a_0=0.36$ Å with the difference between the ionic radius r_{Na} of Na^+ and that, r_{Li}, of Li^+. The value for $r_{\mathrm{Na}}-r_{\mathrm{Li}}$ determined from the Goldschmidt radii is 0.35 Å, the Pauling value is 0.23 Å and the corrected value is 0.20 Å.[21] $\Delta_{\mathrm{Na}}-\Delta_{\mathrm{Li}}$ is approximately equal to the largest value in this range. A certain correlation is expected (the ions will "push" the molecule ion away by an amount essentially equal to their "hard-sphere" radii minus a compression distance) and observed here, but other effects, e.g., the interaction with other neighboring ions, must also be taken into account in making a detailed comparison.

Using the value $R=3.6$ a.u., we have also performed a displacement calculation for the lithium A ions. In this, we have assumed that these ions remain in the YZ plane. Although this is unlikely because of the association, we have still reduced the discrepancy between theory and experiment from 40 to 4%, with the best-fit displacement $\Delta=0.14a_0\hat{Y}+0.10a_0\hat{Z}$. In the lithium B case, discrepancies were brought below 1%.

We note that all but the lithium K and fluorine T nuclei have a negative experimental contact interaction. Large negative values occur for the XY (nodal) plane nuclei; this was also the case for the V_K and V_{KA} centers studied by ENDOR[9–12] and can be explained if exchange polarization of the F_2^- molecule-ion closed-shell orbitals by the unpaired electron is taken into account.[18]

V. CONCLUSION AND DISCUSSION

The ENDOR study described in this paper has proven that the H center in LiF consists of an F_2^- molecule ion that is on an F^- lattice site, oriented in a [110] direction, and associated with a Na^+ impurity as shown in Fig. 1. Hyperfine constants for 10 sets of neighboring nuclei have been determined from the experimental data using a rigorous spin-Hamiltonian diagonalization technique.

An association in the H center with a foreign impurity is consistent with the purity dependence observed for the production rate of this center (see Sec. II and Ref. 4). We have not been able to produce H centers in high-purity Harshaw LiF material by x irradiation but could produce it in reagent-grade material. Since an associated H center was not expected, an ENDOR study was not performed on Na^+-doped material; the production of H centers in such material has been observed.[22] Attempts[7,8] have been made without success to produce H centers in high purity LiF by x irradiation at 4.2°K and by 4.5-MeV electron bombardment at liquid-nitrogen temperatures (sample temperature below 90°K).

No ESR signals from an intrinsic [110] H center are observed in LiF down to He temperatures. The intrinsic defect in LiF is the [111] defect[7,8] stable below approximately 60°K.

It is possible that the ([110]) H centers in KCl and KBr are intrinsic defects. However, it is now believed[23] that in KCl, the V_1 centers, to which H centers are converted on thermal bleaching and from which H centers are generated optically, are H centers of the structure of the KW model but associated with a Na^+ impurity.

It is to be noted that the association in the H center in LiF is with an impurity ion larger than the Li^+ host ion. Previous associations of color centers with impurities (e.g., F_A,[24] V_K, and V_1[23]) have been with smaller impurities (e.g., Na^+ in potassium halides). Past attempts[11] to produce an association between the V_K center and Na^+ impurities in LiF have been unsuccessful.

ACKNOWLEDGMENTS

We have benefitted from illuminating discussions with I. Bass, D. F. Daly, R. Gazzinelli, and R. Marske.

[21] B. S. Gourary and F. J. Adrian, in *Solid State Physics*, edited by F. Seitz and D. Turnbull (Academic Press Inc., New York, 1960), p. 127.

[22] D. F. Daly and Y. Hou Chu (private communication).

[23] C. J. Delbecq *et al.*, Phys. Rev. **154**, 866 (1967); F. J. Keller and F. W. Patten, Bull. Am. Phys. Soc. **14**, 325 (1969); D. Schoemaker *et al.*, *ibid.* **14**, 325 (1969).

[24] F. Luty, Z. Physik **165**, 17 (1961); R. L. Mieher, Phys. Rev. Letters **8**, 362 (1962).

Among these colleagues, we especially thank I. Bass for the use of his computer programs and D. F. Daly for the use of his computer programs and for the performance of the fluorine D and D' dipole-dipole hyperfine constant calculations. We also thank several of the personnel of the Columbia Radiation Laboratory for assistance.

APPENDIX: TECHNIQUE FOR DETERMINATION OF HYPERFINE CONSTANTS

In the technique for determining the hyperfine constants for the ENDOR nuclei, a nuclear type (i.e., a γ_n) and a set of hyperfine constants are assumed, and these parameters are put into the spin Hamiltonian [Eq. (3)]. For a particular orientation of $\mathbf{H}_0$, the matrix of this Hamiltonian in a chosen set of base states is calculated and diagonalized on a computer; the actual value of H_0 used for ENDOR data at this orientation is used in the evaluation. The energy-level scheme is then set up from the eigenvalues and the frequency of a particular ENDOR transition calculated (all on a computer). This is repeated for several orientations of $\mathbf{H}_0$. The hyperfine constants are then varied until the calculated angular dependence of ENDOR frequency is fitted to the experimental data.

The base states used are the 16-dimensional set

$$|m_S,I^{(12)},m_{12},m\rangle \equiv |m_S,I^{(12)},m_{12}\rangle|I,m\rangle,$$

where the $|m_S,I^{(12)},m_{12}\rangle$ were already defined in Eq. (2), $\mathbf{I}$ is quantized along $\mathbf{H}_0$, and we keep in mind that $|I^{(34)},m_{34}\rangle = |0,0\rangle$.

We consider the spin-Hamiltonian matrix elements for the case when the plane of rotation of $\mathbf{H}_0$ is a principal plane of $\mathbf{T}^{(12)}$ but does not contain any principal axes of $\mathbf{A}$. (The case when it does is treated in Ref. 11; the present authors used computer programs prepared for that analysis when such cases arose for the H center.) Assume rotation of $\mathbf{H}_0$ in the YZ plane. Figure 6 indicates the $\mathbf{T}^{(12)}$ principal-axis system XYZ, the magnetic field principal-axis system $X'Y'Z'$ (in which the X' axis is parallel to the X axis and in which the Z' axis is along $\mathbf{H}_0$), and the ENDOR nucleus hyperfine-tensor principal-axis system xyz. The orientation of the xyz system is described by the Euler angles Θ, Ψ, and Φ.

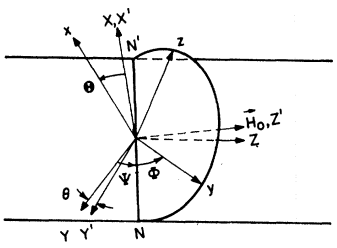

FIG. 6. Diagram showing the Euler angles Θ, Ψ, and Φ which describe the orientation of the nuclear principal-axis system xyz with respect to the H-center principal-axis system XYZ. NN' is the line of nodes. The magnetic field system $X'Y'Z'$ is defined so that $\hat{X}'$ is parallel to $\hat{X}$ and $\hat{Z}'$ to $\mathbf{H}_0$. The angle θ is, as usual, the angle between $\mathbf{H}_0$ and the Z axis.

The $\mathcal{H}_{\text{ESR}}$ component of $\mathcal{H}$ is already diagonal in $|I,m\rangle$ since it contains no $\mathbf{I}$ terms; its matrix elements have already been given for the same base states in Table II of Ref. 11. Calculation of the matrix elements of $\mathcal{H}_{\text{ENDOR}}$ is facilitated if we express the operators $\mathbf{S}$ and $\mathbf{I}$ in terms of components S_X', S_Y', S_Z' and I_X', I_Y', I_Z', respectively, in the $X'Y'Z'$ system. The nuclear Zeeman term then becomes simply $-\gamma_n H_0 I_Z'$. If the transformation from the principal-axis system xyz of $\mathbf{A}$ to the $X'Y'Z'$ system (Fig. 6) is expressed by the 3×3 matrix D, we can write for the components of $\mathbf{I}$ and $\mathbf{S}$ in Eq. (8):

$$I_i=\sum_{k=1}^{3} D_{ik}I_k', \quad S_i=\sum_{t=1}^{3} D_{it}S_t',$$

with $i=1$, 2, and 3. Substituting these in Eq. (8), we get

$$\mathbf{I}\cdot\mathbf{A}\cdot\mathbf{S}=\sum_{k,t=1}^{3} C_{kt}I_k'S_t', \tag{A1}$$

where

$$C_{kt}=\sum_{i=1}^{3} D_{ik}D_{it}A_i. \tag{A2}$$

The calculation of the D_{ij} coefficients as a function of the angles θ, Θ, Φ, and Ψ is a straightforward problem in trigonometry and the results, given in Ref. 5(a), are lengthy and will not be given here. Once the D_{ij} coefficients are calculated, the C_{kt} coefficients can be calculated by substitution in Eq. (A2). The resulting 16×16 matrix will be complex and Hermitian but can be handled[11] by available computer subroutines if, instead of diagonalizing the matrix $\mathcal{H}=\mathcal{R}+i\mathcal{I}$, where $\mathcal{R}$ and $\mathcal{I}$ are real, we diagonalize the 32×32 real symmetric matrix

$$\begin{pmatrix} \mathcal{R} & \mathcal{I} \\ -\mathcal{I} & \mathcal{R} \end{pmatrix}.$$

The matrix $\mathcal{R}$ is given in Table IV of Ref. 11, where we note that the 3×3 matrix W becomes our matrix C multiplied by $\frac{1}{4}$. The antisymmetric matrix $\mathcal{I}$ has the following nonzero elements above the diagonal:

$$\begin{aligned}\langle 1a|\mathcal{I}|1b\rangle &= \langle 1a|\mathcal{I}|5a\rangle = -\langle 1b|\mathcal{I}|5b\rangle = \langle 2a|\mathcal{I}|2b\rangle \\ &= \langle 2a|\mathcal{I}|6a\rangle = -\langle 2b|\mathcal{I}|6b\rangle = \langle 3a|\mathcal{I}|3b\rangle \\ &= \langle 3a|\mathcal{I}|7a\rangle = -\langle 3b|\mathcal{I}|7b\rangle = \langle 4a|\mathcal{I}|4b\rangle \\ &= \langle 4a|\mathcal{I}|8a\rangle = -\langle 4b|\mathcal{I}|8b\rangle = -\langle 5a|\mathcal{I}|5b\rangle \\ &= -\langle 6a|\mathcal{I}|6b\rangle = \langle 7a|\mathcal{I}|7b\rangle = -\langle 8a|\mathcal{I}|8b\rangle = \tfrac{1}{4}C_{13},\end{aligned}$$

and

$$\langle 1a|\mathcal{I}|5b\rangle = \langle 2a|\mathcal{I}|6b\rangle = \langle 3a|\mathcal{I}|7b\rangle = \langle 4a|\mathcal{I}|8b\rangle = \tfrac{1}{2}C_{12},$$

where the base vectors $|1a\rangle$, $|1b\rangle$, $|2a\rangle\cdots|8b\rangle$ are defined in Ref. 11. Rotations in the XZ plane can be handled with the same $\mathcal{H}$ matrix if the tensors $\mathbf{T}^{(12)}$ and $\mathbf{g}$ have their principal values properly exchanged and angles are properly redefined.